Human spectrin Src homology 3 domain binding protein 1 regulates macropinocytosis in NIH 3T3 cells

Jiliu Xu[1], **Dorota Ziemnicka**[1], **George S. Merz**[2], and **Leszek Kotula**[1,*]

[1]Laboratory of Molecular Neurobiology, New York State Institute for Basic Research in Developmental Disabilities, Staten Island, NY 10314, USA

[2]Laboratory of Digital Microscopy, New York State Institute for Basic Research in Developmental Disabilities, Staten Island, NY 10314, USA

SUMMARY

Macropinocytosis is an endocytic process that occurs through non-clathrin coated vesicles larger than 0.2 μm in diameter. Although macropinocytic vesicles are readily visualized in cultured cells by the introduction of fluorescent, water-soluble dyes into the culture medium, protein markers associated with this type of vesicles have not yet been well defined. Here, we report that human spectrin SH3 domain binding protein 1, or Hssh3bp1, associates with macropinosomes in NIH 3T3 fibroblasts. Hssh3bp1 macropinosomes are heterogeneous in morphology and size, do not endocytose transferrin and are resistant to brefeldin A treatment. Cytochalasin D, and wortmannin block endocytosis of fluorescent dyes into the Hssh3bp1 macropinosomes and dramatically affect their morphology. Overexpression of Hssh3bp1-green fluorescent protein abolished fusion of vesicles resulting in a decreased endocytosis of fluorescence dyes, thus suggesting a potential regulatory role of Hssh3bp1 in macropinocytosis. In the macropinosomes of NIH 3T3 cells, Hssh3bp1 associates with a 200-kDa protein that crossreacts with a monoclonal antibody to the erythroid α-spectrin SH3 domain. Thus macropinosomes in cells may contain a spectrin-like protein.

Keywords

Endosome; Membrane protein; Pinocytosis; Spectrin; Src homology domain

INTRODUCTION

Spectrin is an actin-crosslinking protein originally identified in red blood cells. Spectrin-actin complexes interact with several accessory proteins such as ankyrin to form the so-called 'membrane skeleton' (reviewed by Bennett and Gilligan, 1993; Tse and Lux, 1999). Identification of spectrin mutations in different forms of hereditary anemia indicates the critical role of spectrin in maintaining integrity and shape of the erythroid plasma membrane. Recently, the functional paradigm of the spectrin-based membrane skeleton has been extended to membranes of intracellular organelles such as Golgi (Beck et al., 1994;

---

[*]Author for correspondence (kotulal@rcn.com).

Devarajan et al., 1996; Beck et al., 1997; Stankewich et al., 1998), endoplasmic reticulum (Zhou et al., 1997) and lysosomes (Hoock et al., 1997). Microinjection of recombinant erythroid ankyrin blocks clathrin-dependent endocytosis of low-density lipoprotein, suggesting a role for the spectrin membrane skeleton in endocytic processes in nonerythroid cells (Michaely et al., 1999).

Endocytosis is a process involving the uptake of large particles, fluids and macromolecules from the outside to the inside of a cell. The latter, called pinocytosis, often involves membrane-bound receptors and occurs through clathrin-coated vesicles (reviewed by Lamaze and Schmid, 1995; Swanson and Watts, 1995). However, treatments that block clathrin-dependent endocytosis only such as hypertonicity (Daukas and Zigmond, 1985; Heuser and Anderson, 1989), K^+ depletion (Larkin et al., 1986), cytosolic acidification (Sandvig et al., 1987), and expression of dynamin mutants (Damke et al., 1994; Damke et al., 1995) do not completely block cellular endocytosis, indicating the existence of clathrin-independent mechanisms of this process.

Non-clathrin dependent mechanisms of endocytosis include macropinocytosis which occurs through large, vesicles of variable size (0.2–2.0 μm), that can be visualized in the cell following addition of fluorescent dyes into the culture medium. Macrophages and tumor cell lines show high macropinocytic activity, which can be upregulated by the treatment of cells with growth factors such as epidermal growth factor (Haigler et al., 1979; Hewlett et al., 1994), platelet-derived growth factor (Davies and Ross, 1978), insulin-like derived growth factor-1 (Miyata et al., 1988), macrophage colony-stimulating factor (Racoosin and Swanson, 1992); and by treatment with mitogenic agents such as phorbol esters and diacylglycerol (West et al., 1989). Nocodazole (Racoosin and Swanson, 1992) and inhibitors of PI-3-kinase such as wortmannin and LY294002 appear to inhibit the process (Araki et al., 1996). Macropinocytosis is often preceded by membrane ruffling (Bar-Sagi et al., 1986), which is an actin cytoskeleton-dependent event inhibited by cytochalasin D (Allison et al., 1971).

The structural components of macropinocytic vesicles are not well defined. In this study, we determined that Hssh3bp1, a protein binding to the spectrin SH3 domain and Abl tyrosine kinase (Ziemnicka-Kotula et al., 1998), associates with macropinocytic vesicles in NIH 3T3 cells. Overexpression of Hssh3bp1-GFP decreased endocytosis of a fluorescent dye raising the possibility of a regulatory role for Hssh3bp1 in macropinocytosis. In the NIH 3T3 macropinosomes, Hssh3bp1 associates with a 200-kDa protein that crossreacts with a mAb to the erythroid α-spectrin SH3 domain. Thus macropinosomes might contain a spectrin-like membrane skeleton similar to that of erythrocytes.

MATERIALS AND METHODS

Reagents and antibodies

BFA, transferrin, wortmannin, nocodazole, cytochalasin D, and bafilomycin were from Sigma (St Louis, MO). Wheat germ agglutinin-Texas red (WGA-TR) conjugate and Alexa 594 were from Molecular Probes (Eugene, OR); Lipofectamine Plus from Life Technologies

(Rockville, MD); LY294002 was from Calbiochem (San Diego, CA); and Protein A Trisacryl from Pierce (Rockford, IL).

Antibodies to the following were obtained commercially: transferrin and β tubulin were from (Sigma); clathrin (clone X22), calnexin, and calreticulin (Affinity Bioreagents, Inc., Golden, CO); Lamp 1 (Developmental Studies Hybridoma Bank, Univ. of Iowa, Iowa City, IA); and Rab 5a (Santa Cruz Biotechnology, Santa Cruz, CA). Polyclonal antibodies to mannosidase II and to mannose-6-phosphate receptor were obtained from Dr Kelley W. Moremen (Univ. of Georgia, Athens, GA), and Dr Janet Larkin (Barnard College, Columbia University, New York, NY), respectively.

mAb 17C7, raised to the recombinant α spectrin SH3 domain (plasmid GST-E-SH3; Ziemnicka-Kotula et al., 1998), and mAb 4E2, raised to the recombinant Hssh3bp1 (plasmid C2; Ziemnicka-Kotula et al., 1998) and detecting residues 373–388 of the protein, were produced at our Institute for Basic Research in Developmental Disabilities Antibody Facility using standard techniques. mAb 17C7 did not crossreact with the recombinant human fodrin SH3 domain, and showed no fodrin-specific immunostaining in NIH 3T3 cells. Polyclonal antibody Ab-2 was raised against a synthetic peptide containing the C-terminal eight amino acids of Hssh3bp1. Secondary antibodies were from Jackson ImmunoResearch, Inc. (West Grove, PA) and from Molecular Probes (Eugene, OR).

Cell culture and transfections

NIH 3T3 cells (obtained from ATCC, Rockville, MD) were grown on coverslips in DMEM supplemented with 10% bovine calf serum. Cells were transfected with expression plasmids using Lipofectamine Plus Reagent according the manufacturer's instructions. At 22 hours post-transfection, cells were processed for indirect immunofluorescence as described (Ziemnicka-Kotula et al., 1998). In transfection experiments the following plasmids were used: NG-1, expressing isoform 1 of Hssh3bp1; N3-1, expressing isoform 1 of Hssh3bp1 fused to GFP (Ziemnicka-Kotula et al., 1998); and pEGFP-N3 (Clontech, Palo Alto, CA) were used in transfections. Coverslips were mounted in 0.1% phenylenediamine in 90% glycerol and 10% PBS.

Uptake of fluorescent markers and transferrin

Uptake of the fluorescent markers WGA-TR (at 10 μg/ml) and Alexa 594 (1 mg/ml) was monitored at several time points (from 5 minutes up to 2 hours after addition of the marker to medium) following fixation of cells with methanol. Uptake of transferrin was observed following staining with polyclonal antibody to transferrin.

Cells were treated with wortmannin (0.2 μM), LY294002 (50 μM) or nocodazole (33 μM) as described (Araki et al., 1996). Cytochalasin D was used at 3 μM. Incubation of cells with BFA (5 μg/ml) was for 10 minutes at 37°C.

Vesicle size measurements, confocal microscopy and quantitation of WGA-TR uptake in Hssh3bp1-GFP-transfected cells

Hssh3bp1 vesicle size was measured in NIH 3T3 cells immunostained with mAb 4E2 followed by incubation with anti-mouse Alexa 488 conjugate. Representative images from several cells were generated using a Nikon PCM 2000 Confocal Imaging System. Vesicle size was estimated using Simple 32 Image Analysis Software (C-imaging, Cranberry Township, PA).

Cells transiently transfected with Hssh3bp1-GFP fusion protein were grown on coverslips mounted in Sykes-Moore chambers and maintained at 37°C on the heated stage of a Nikon TE Eclipse 200 inverted microscope coupled to the imaging system described above. High-resolution images (1024×1024 pixels) were collected using a ×60 NA 1.4 objective. Representative images from live cells and measurements of WGA-TR fluorescence endocytosed by cells were obtained after a 5-minute uptake of the marker at 37°C and a single wash with medium. Images from cells transfected with Hssh3bp1-GFP, GFP and nontransfected cells were collected at 1 hour from initial addition of the marker to medium. Quantitation of endocytosed fluorescence was performed using Simple 32 Image Analysis Software (C-imaging, Cranberry Township, PA). Statistical analysis was performed using Statistica Software (StatSoft, Inc. Tulsa, OK). Covariance analysis, ANCOVA, with a cell image area as a covariate indicated that differences in endocytosis of fluorescent WGA among the groups did not depend on the image area.

Subcellular fractionation and immunoprecipitation

Subcellular fractionation of NIH3T3 cells was performed as described (Gorvel et al., 1991; Aniento et al., 1996). An early endosomal fraction was identified by the highest activity of endocytosed HRP after a 5-minute uptake at 37°C (not shown).

Immunoprecipitation was performed as described (Fazioli et al., 1992). Briefly, cells grown on 175-cm^2 flasks were washed once and scraped in ice-cold PBS containing 500 μM sodium vanadate and 4 mM diisopropylfluorophosphate. Cells were then lysed in lysis buffer (50 mM HEPES, pH 7.5, 1% Triton X-100, 50 mM NaCl, 5 mM EGTA, 50 mM sodium fluoride, 20 mM sodium pyrophosphate, 1 mM sodium vanadate, 2 mM PMSF, 8 mM diisopropylfluorophosphate) at a concentration of 1×10^8/ml. Lysates were processed for immunoprecipitation using Protein A Trisacryl as described (Fazioli et al., 1991) and immunoprecipitates were washed extensively with buffer containing 0.1% Triton X-100, 20 mM HEPES, and 50 mM NaCl, followed by solubilization in 2× Laemmli sample buffer. Western blotting was performed as described (Ziemnicka-Kotula et al., 1998).

RESULTS

Hssh3bp1 and Hssh3bp1-GFP associate with cytoplasmic vesicle-like structures resistant to BFA treatment

NIH 3T3 fibroblasts stained with monoclonal antibody (mAb) 4E2 to Hssh3bp1 revealed a punctate, vesicular-like cytoplasmic staining pattern (Fig. 1a) similar to that of cells expressing relatively low levels of Hssh3bp1-green fluorescent protein (GFP) (Ziemnicka-

Kotula et al., 1998 and Fig. 1b) or recombinant wild-type Hssh3bp1 (Fig. 1c). However, vesicles containing recombinant forms of the protein appeared to be less concentrated in the perinuclear region of cells and had a more uniform round-like shape than vesicles stained with the mAb 4E2 to endogenous Hssh3bp1, subsequently referred to as Hssh3bp1 (compare Fig. 1b,c,g to Fig. 1a and e). To obtain similar immunostaining intensities of vesicles with mAb 4E2 in cells transfected with the recombinant wild-type Hsshb3p1 (Fig. 1c) or Hssh3bp1-GFP (not shown) to those observed in nontransfected cells (Fig. 1a) it is necessary to dilute the antibody 10–40 times. Therefore, it is likely that the transfected cells overexpress Hssh3bp1.

Immunofluorescence studies using organelle-specific antibodies revealed no colocalization of either Hssh3bp1 or Hssh3bp1-GFP vesicles with calreticulin and calnexin, markers of endoplasmic reticulum (not shown). The Hssh3bp1 and Hssh3bp1-GFP staining pattern did not change upon brefeldin A (BFA) treatment (Fig. 1e–h) and did not coincide with staining for mannosidase II, a Golgi marker, either before or after the treatment. Thus, Hssh3bp1 and Hssh3bp1-GFP do not associate with Golgi or with the BFA-sensitive endosomal-lysosomal system (Lippincott-Schwartz et al., 1991). Consistent with these results, Hssh3bp1 (Fig. 2a) and Hssh3bp1-GFP (not shown) did not associate with late endosomes, as indicated by the lack of colocalization with mannose-6-phosphate receptor. In addition the morphology of Hssh3bp1 (not shown) and Hssh3bp1-GFP (Fig. 2b) vesicles was not affected by bafilomycin A treatment, which prevents acidification of lysosomes and results in their enlargement. Costaining of Hssh3bp1-GFP and clathrin (Fig. 2c) indicated that Hssh3bp1-GFP vesicles do not contain a clathrin coat.

In subsequent experiments we examined whether Hssh3bp1 and Hssh3bp1-GFP associate with early endosomal compartments. Hssh3bp1 colocalized with the majority of vesicles containing endocytosed wheat germ aglutinin-Texas red (WGA-TR) conjugate (Fig. 2d–f) or other water-soluble fluorescent dyes such as Alexa 594 (not shown). It was observed that Hssh3bp1 did not associate with early or recycling endosomes since it did not colocalize with Rab5 (not shown) or with the majority of vesicles containing endocytosed transferrin (Fig. 2g–i). The colocalization of Hssh3bp1 with WGA-TR occurred within the 5-minute period after the addition of WGA-TR to the tissue culture medium, suggesting association of Hssh3bp1 with rapidly forming endosomal vesicles. No colocalization of Hssh3bp1-GFP with endocytosed WGA-TR, transferrin, or with Rab 5 was observed (not shown). In addition, lower amounts of endocytosed fluorescence associated with cells transfected with Hssh3bp1-GFP was observed (see below).

Colocalization experiments using Hssh3bp1-specific mAb 4E2 and Hssh3bp1-GFP and antibodies to organelles yielded identical results. This and the fact that endogenous Hssh3bp1 vesicles and Hssh3bp1-GFP vesicles are resistant to BFA treatment, suggest that both endogenous Hssh3bp1 and Hssh3bp1-GFP localize to the same intracellular compartment. However, no colocalization with endocytosed WGA-TR of Hssh3bp1-GFP vesicles, and lower amounts of endocytosed fluorescence associated with transfected cells suggested that the endocytic compartment responsible for uptake of WGA-TR might be functionally altered by overexpression of the Hssh3bp1-GFP fusion protein.

Size measurements and functional assays identify Hssh3bp1 vesicles as macropinosomes

The colocalization of Hssh3bp1 vesicles with endocytosed fluorescent markers but not with endocytosed transferrin, and the resistance to BFA treatment are consistent with that of macropinosomes (Hewlett et al., 1994). The Hssh3bp1 vesicles also apeared to be larger and more heterogenous in size and shape than clathrin-coated vesicles (Fig. 2c). Measurements of endogenous Hssh3bp1 vesicles indicated the vesicles a size range of 0.5–2 μm in diameter (Fig. 3), consistent with that observed for macropinocytic vesicles (Hewlett et al., 1994). The average diameter of Hssh3bp1 vesicles was 1.30±0.59 μm.

Addition of wortmannin (Fig. 4c,d) or LY294002 (not shown), two PI-3 kinase inhibitors or cytochalasin D (Fig. 4e,f), an actin filament depolymerizing agent, to the culture medium prevented endocytosis of the fluorescent marker Alexa 594. These treatments also altered morphology of the vesicles. Moreover, treatment of cells with the microtubule-depolymerizing agent nocodazole dramatically altered the morphology and organization of Hssh3bp1 vesicles (Fig. 5a and b). These results are consistent with the functional properties described for macropinosomes in macrophages (Araki et al., 1996; Allison et al., 1971). On the other hand, the morphology of the Hssh3bp1-GFP vesicles in transfected cells was not affected by nocodazole (Fig. 5c and d), suggesting that the functional relationship of Hssh3bp1-GFP vesicles to microtubules differs from that of Hssh3bp1 vesicles.

Overexpression of Hssh3bp1-GFP decreases macropinocytic uptake of fluorescent markers in NIH 3T3 cells

Cells transfected with Hssh3bp1-GFP appeared to endocytose less WGA-TR and less Alexa 594 (not shown) than nontransfected cells. Quantitation of endocytosed fluorescence in cells (Fig. 6A and B) indicated that cells transfected with Hssh3bp1-GFP endocytosed about 50% less fluorescence than cells transfected with GFP only ($P<0.001$) or about 60% less than nontransfected cells ($P<0.001$). Thus overexpression of Hssh3bp1-GFP specifically decreased endocytosis of WGA-TR in transfected NIH 3T3 cells. No colocalization of Hssh3bp1-GFP with the WGA-TR-containing vesicles was observed.

To gain an insight into why Hssh3bp1-GFP vesicles do not take up WGA-TR we examined vesicles in live cells. Images of live cells transfected with Hssh3bp1-GFP were collected from several cells every 40 seconds for 10–30 minutes and vesicles were analyzed frame-by-frame. Hssh3bp1-GFP vesicles moved but only over relatively short distances (Fig. 6C). Vesicles often moved towards each other and overlapped, suggesting a rotation or a movement in a different focal plane. Lack of formation of larger structures and the fact that vesicles quickly separated suggest that they do not fuse with each other. Hssh3bp1-GFP vesicles also did not take up the fluorescent WGA, indicating that they also do not fuse with WGA-TR vesicles. This is in contrast to endogenous Hssh3bp1 vesicles which clearly took up the fluorescent marker (see Fig. 2d–f) and likely fuse with vesicles containing fluorescent markers or bud from the plasma membrane. Observation of WGA-TR-labeled vesicles in live cells, the majority of which represent Hssh3bp1 vesicles (Fig. 2d–f), indicates substantial morphological changes in the vesicles within time, movement of vesicles towards the perinuclear area of the cell, and possible budding or fusion events (Fig. 6C).

Formation of short tubular structures with long axis pointing towards the perinuclear area can be often observed.

Hssh3bp1 and Hssh3bp1-GFP associates with a 200-kDa protein in NIH 3T3 cells macropinosomes

Hssh3bp1 was cloned based on its interaction with the α-spectrin SH3 domain and contains the spectrin SH3 domain-specific binding site. In NIH 3T3 cells, Hssh3bp1-GFP vesicles stain with the polyclonal antibody to human spectrin (Ziemnicka-Kotula et al., 1998), suggesting that the vesicles contain an α-like spectrin (β-spectrin does not contain an SH3 domain). Several mAbs specific to the α-spectrin SH3 domain were used to characterize this protein. mAb 17C7 reacted with the mouse erythroid α-spectrin and with a 200-kDa protein in NIH 3T3 cells, and in mouse cerebellum (Fig. 7), a tissue known to express erythroid α spectrin (Riederer et al., 1986). The mAb 17C7 immunostaining pattern in NIH 3T3 cells was very similar to that observed with antibodies to Hssh3bp1 and coincided with vesicles containing endocytosed WGA-TR (Fig. 8). These data suggest that Hssh3bp1 and the 200-kDa protein are present in the same vesicles in NIH 3T3 cells. Subcellular fractionation of NIH 3T3 cells indicated enrichment of both proteins in the early endosomal fraction (Fig. 7).

To determine whether Hssh3bp1 interacts with the 200-kDa protein, immunoprecipitation experiments were carried out using the affinity-purified polyclonal antibody to Hssh3bp1. The 200-kDa protein coprecipitated with Hssh3bp1 in NIH 3T3 cells, and with Hssh3bp1 and Hssh3bp1-GFP in transfected NIH 3T3 cells (Fig. 7). Thus complexes containing Hssh3bp1 or Hssh3bp1-GFP and the 200-kDa protein exist in macropinocytic vesicles in NIH 3T3 cells.

DISCUSSION

Here we present evidence that Hssh3bp1 associates with macropinocytic vesicles in NIH 3T3 cells. The characteristics of Hssh3bp1 vesicles are consistent with the defining criteria for macropinocytic compartments (Swanson, 1989; Hewlett et al., 1994; reviewed by Lamaze and Schmid, 1995; Swanson and Watts, 1995). Specifically, Hssh3bp1 vesicles do not have a clathrin-coat, are heterogenous in size, and, on average, are much larger than clathrin-coated vesicles. Hssh3bp1 vesicles associate with endocytosed fluorescent dyes, do not contain endocytosed transferrin, and are resistant to BFA treatment (West et al., 1989; Hewlett et al., 1994).

Treatment of cells with wortmannin/LY294002 and cytochalasin D affected morphology of Hssh3bp1 vesicles and impaired endocytosis of fluorescent dyes. These agents probably act by two independent mechanisms. The wortmannin/LY294002 treatment inhibits PI-3 kinase (Vlahos et al., 1994) and blocks membrane ruffling by inhibiting PI3-kinase-Rac1 signaling (Ridley et al., 1992; Hawkins et al., 1995). Since membrane ruffling precedes macropinocytosis and a macropinocytic-ready compartment (in the form of Hssh3bp1 vesicles) already exists in cells, PI3-kinase must initiate or control a step that connects a membrane ruffle with the Hssh3bp1 vesicle. Observations by Araki et al. (Araki et al., 1996) in macrophages indicate that PI3-kinase does not block formation of membrane pseudopods but rather does block closure of membrane invaginations into macropinosomes or

phagosomes. Our data suggest that such membrane invaginations are likely to fuse with an Hssh3bp1 vesicle or acquire Hssh3bp1 to form a functional macropinosome. Depolymerization of actin filaments by cytochalasin D, on the other hand, blocks formation of membrane ruffles so that the transport through Hssh3bp1 macropinosomes cannot occur.

A recent study implicates Hssh3bp1 in the Ras-PI3-kinase-Rac signaling. Isoform 2 of Hssh3bp1 is identical to E3b1 (Ziemnicka-Kotula et al., 1998), a protein binding to the Eps8 SH3 domain (Biesova et al., 1997). E3b1 forms a tripartate complex with Eps8 and Sos-1 which in turn inhibits Rac-specific guanine exchange factor activity in vitro (Scita et al., 1999). Consequently, microinjection of antibodies to E3b1 inhibits membrane ruffle formation due to PDGF stimulation (Scita et al., 1999) by affecting the Rac signaling pathway.

Movement and organization of Hssh3bp1 macropinosomes are likely to be controlled by microtubules since nocodazole treatment dramatically affected the morphology of Hssh3bp1 vesicles. Patchy staining of Hssh3bp1 vesicles in nocodazole-treated cells suggests aggregation of vesicles and/or formation of large vacuolar structures. These structures did not participate in endocytic uptake (data not shown), consistent with findings in macropinocytic vesicles of macrophages (Racoosin and Swanson, 1992). It is likely that lack of microtubules in nocodazole treated cells prevents movement of vesicles required for proper fusions of vesicles, similar to observations in endosomal vesicles (Matteoni and Kreis, 1987; Gruenberg et al., 1989). Hssh3bp1-GFP vesicles lost their ability to fuse probably due to an altered interaction with microtubules. The functional association of microtubules with Hssh3bp1-GFP vesicles differs from that of endogenous Hssh3bp1 vesicles since the morphology of Hssh3bp1-GFP vesicles was not affected by nocodazole. This did not depend on the position of GFP in the fusion protein (nocodazole did not affect the morphology of vesicles containing either N-terminal or C-terminal fusions of Hssh3bp1) and was the same in cells expressing wild-type Hssh3bp1 (not shown). Vesicles containing expressed Hssh3bp1-GFP or wild-type Hssh3bp1 (not shown) did not take up fluorescent markers presumably because they were unable to fuse with vesicles containing fluorescent markers. mAb 4E2 to Hssh3bp1 associates with a majority of WGA-TR loaded vesicles, therefore, we used WGA-TR as a marker of Hssh3bp1 vesicles in live cells. In contrast to Hssh3bp1-GFP vesicles, WGA-TR vesicle movement towards the perinuclear area of cells can be easily observed. The movement is evident in times as short as 7 seconds (not shown); the vesicles often disappear from focal plane. Formation of short tubular structures extending towards the perinuclear region of cells is characteristic of WGA-TR vesicles. Since not all WGA-TR vesicles contain Hssh3bp1, but all Hsshb3p1 vesicles uptake WGA-TR, it is possible that Hssh3bp1 vesicles represent a subset of WGA-TR vesicles with some specific properties. WGA-TR uptake experiments in cells microinjected with anti-Hssh3bp1 antibodies or in cells stably transfected with Hssh3bp1 will facilitate a better understanding of a possible role of the protein in vesicle movement and fusion. Expression of Hssh3bp1-GFP decreased the endocytic uptake by 50% in comparison to GFP-transfected cells, thus suggesting a potential regulatory role for Hssh3bp1 in macropinocytosis. Reduction of endocytic uptake was observed in the vast majority of Hssh3bp1-transfected cells and it is likely to be due to an overexpression of the protein in transiently transfected cells.

Hssh3bp1 interacts with a protein, 200-kDa, in the NIH 3T3 macropinosomes. Since the 200-kDa protein was detected with mAb 17C7 raised to the α-spectrin SH3 domain, the protein must contain an SH3 domain. This SH3 domain is a likely binding site of Hssh3bp1, since overexpression of Hssh3bp1 blocks staining of vesicles in NIH 3T3 cells with this antibody but not with the polyclonal antibody to the spectrin SH3 domain (data not shown). Thus, both endogenous Hssh3bp1 and Hssh3bp1-GFP target vesicles that contain the 200-kDa spectrin-like protein. Whether the 200-kDa protein contains spectrin-like repeat units (Speicher and Marchesi, 1984) and is another α-spectrin isoform, remains to be determined. In any case, the mAb 17C7 to the 200-kDa protein may serve as a marker of macropinocytic vesicles.

The possibility that macropinocytic vesicles contain a spectrin-like membrane skeleton is strengthened by identification of a specific Golgi spectrin (Beck et al., 1994; Stankewich et al., 1998), and by the presence of ankyrin isoforms in several intracellular organelles such as lysosomes (Hoock et al., 1997), endoplasmic reticulum (Zhou et al., 1997), and Golgi (Beck et al., 1997). Erythroid ankyrin may be important for clathrin-dependent endocytosis (Michaely et al., 1999). In a model analogous to the model of the red cell membrane skeleton, an ankyrin isoform would link spectrin to an organelle membrane either directly or through a secondary protein(s). The spectrin-based membrane skeleton has been proposed to play a role as protein sorting machinery similar to the role of clathrin (Beck et al., 1994; reviewed by Beck and Nelson 1996; De Matteis and Morrow, 1998). In this scenario, complexes of ankyrin and spectrin isoforms would provide binding sites for specific regulatory proteins i.e. Hssh3bp1, required for the function of a particular membrane-containing organelle.

Acknowledgments

References

Allison AC, Davies P, De Petris S. Role of contractile microfilaments in macrophage movement and endocytosis. Nature New Biol. 1971; 232:153–155. [PubMed: 4937093]

Aniento F, Gu F, Parton RG, Gruenberg J. An endosomal beta COP is involved in the pH-dependent formation of transport vesicles destined for late endosomes. J Cell Biol. 1996; 133:29–41. [PubMed: 8601610]

Araki N, Johnson MT, Swanson JA. A role for phosphoinositide 3-kinase in the completion of macropinocytosis and phagocytosis by macrophages. J Cell Biol. 1996; 135:1249–1260. [PubMed: 8947549]

Bar-Sagi D, Feramisco JR. Induction of membrane ruffling and fluid-phase pinocytosis in quiescent fibroblasts by ras proteins. Science. 1986; 233:1061–1068. [PubMed: 3090687]

Beck KA, Buchanan JA, Malhotra V, Nelson WJ. Golgi spectrin: Identification of an erythroid α-spectrin homolog associated with the Golgi complex. J Cell Biol. 1994; 127:707–723. [PubMed: 7962054]

Beck KA, Nelson WJ. The spectrin-based membrane skeleton as a membrane protein sorting machine. Am J Physiol. 1996; 270:C1263–1270. [PubMed: 8967424]

Beck KA, Buchanan JA, Nelson WJ. Golgi membrane skeleton: identification, localization and oligomerization of a 195 kDa ankyrin isoform associated with the Golgi complex. J Cell Sci. 1997; 110:1239–1249. [PubMed: 9191047]

Bennett V, Gilligan DM. The spectrin-based membrane skeleton and micron-scale organization of the plasma membrane. Annu Rev Cell Biol. 1993; 9:27–66. [PubMed: 8280463]

Biesova Z, Piccoli C, Wong WT. Isolation and characterization of e3B1, an eps8 binding protein that regulates cell growth. Oncogene. 1997; 14:233–241. [PubMed: 9010225]

Damke H, Baba T, Warnock DE, Schmid SL. Induction of mutant dynamin specifically blocks endocytic coated vesicle formation. J Cell Biol. 1994; 127:915–934. [PubMed: 7962076]

Damke H, Baba T, Van der Bliek AM, Schmid SL. Clathrin-independent pinocytosis is induced in cells overexpressing a temperature-sensitive mutant of dynamin. J Cell Biol. 1995; 131:69–80. [PubMed: 7559787]

Daukas G, Zigmond SH. Inhibition of receptor-mediated but not fluid-phase endocytosis in polymorphonuclear leukocytes. J Cell Biol. 1985; 101:1673–1679. [PubMed: 4055891]

Davies PF, Ross R. Mediation of pinocytosis in cultured arterial smooth muscle and endothelial cells by platelet-derived growth factor. J Cell Biol. 1978; 79:663–671. [PubMed: 103882]

De Matteis MA, Morrow JS. The role of ankyrin and spectrin in membrane transport and domain formation. Curr Opin Cell Biol. 1998; 4:542–549. [PubMed: 9719877]

Devarajan P, Stabach PR, Mann AS, Ardito T, Kashgarian M, Morrow JS. Identification of a small cytoplasmic ankyrin (AnkG119) in the kidney and muscle that binds beta I sigma spectrin and associates with the Golgi apparatus. J Cell Biol. 1996; 133:819–830. [PubMed: 8666667]

Fazioli F, Kim UH, Rhee SG, Molloy CJ, Segatto O, Di Fiore PP. The erbB-2 mitogenic signaling pathway: tyrosine phosphorylation of phospholipase C-gamma and GTPase-activating protein does not correlate with erbB-2 mitogenic potency. Mol Cell Biol. 1991; 11:2040–2048. [PubMed: 1672440]

Fazioli F, Bottaro DP, Minichiello L, Auricchio A, Wong WT, Segatto O, Di Fiore PP. Identification and biochemical characterization of novel putative substrates for the epidermal growth factor receptor kinase. J Biol Chem. 1992; 267:5155–5161. [PubMed: 1347529]

Gorvel PL, Chavrier P, Zerial M, Gruenberg J. Rab5 controls early endosome fusion in vitro. Cell. 1991; 64:915–925. [PubMed: 1900457]

Gruenberg J, Griffiths G, Howell KE. Characterization of the early endosome and putative endocytic carrier vesicles in vivo and with an assay of vesicle fusion in vitro. J Cell Biol. 1989; 108:1301–1316. [PubMed: 2538480]

Haigler HT, McKanna JA, Cohen S. Rapid stimulation of pinocytosis in human carcinoma cells A-431 by epidermal growth factor. J Cell Biol. 1979; 83:82–90. [PubMed: 315944]

Hawkins PT, Eguinoa A, Qiu RG, Stokoe D, Cooke FT, Walters R, Wennstrom S, Claesson-Welsh L, Evans T, Symons M, Stephens L. PDGF stimulates an increase in GTP-Rac via activation of phosphoinositide 3-kinase. Curr Biol. 1995; 5:393–403. [PubMed: 7627555]

Heuser JE, Anderson RGW. Hypertonic media inhibit receptor-mediated endocytosis by blocking clathrin-coated pit formation. J Cell Biol. 1989; 108:389–400. [PubMed: 2563728]

Hewlett LJ, Prescott AR, Watts C. The coated pit and macropinocytic pathways serve distinct endosome populations. J Cell Biol. 1994; 124:689–703. [PubMed: 8120092]

Hoock TC, Peters LL, Lux SE. Isoforms of ankyrin-3 that lack the NH2-terminal repeats associate with mouse macrophage lysosomes. J Cell Biol. 1997; 136:1059–1070. [PubMed: 9060470]

Lamaze C, Schmid SL. The emergence of clathrin-independent pinocytic pathways. Curr Opin Cell Biol. 1995; 7:573–580. [PubMed: 7495578]

Larkin JM, Donzell WC, Anderson RGW. Potassium-dependent assembly of coated pits: new coated pits form as planar clathrin lattices. J Cell Biol. 1986; 103:2619–2627. [PubMed: 2878930]

Lippincott-Schwartz J, Yuan L, Tipper C, Amherdt M, Orci L, Klausner RD. BFA's effects on endosomes, lysosomes, and the TGN suggest a general mechanism for regulating organelle structure and membrane traffic. Cell. 1991; 67:601–616. [PubMed: 1682055]

Matteoni R, Kreis T. Translocation and clustering of endosomes and lysosomes depends on microtubules. J Cell Biol. 1987; 105:1253–1265. [PubMed: 3308906]

Michaely P, Kamal A, Anderson RGW, Bennett V. A requirement for ankyrin binding to clathrin during coated pit budding. J Biol Chem. 1999; 274:35908–35913. [PubMed: 10585476]

Miyata Y, Hoshi M, Koyasu S, Kadowaki T, Kasuga M, Yahara I, Nishida E, Sakai H. Rapid stimulation of fluid-phase endocytosis and exocytosis by insulin, insulin-like growth factor-1, and epidermal growth factor in KB cells. Exp Cell Res. 1988; 178:73–83. [PubMed: 2970395]

Racoosin EL, Swanson JA. M-CSF-induced macropinocytosis increases solute endocytosis but not receptor-mediated endocytosis in mouse macrophages. J Cell Sci. 1992; 102:867–880. [PubMed: 1429898]

Ridley AJ, Paterson HF, Johnston CL, Diekmann D, Hall A. The small GTP-binding protein Rac regulates growth factor-induced membrane ruffling. Cell. 1992; 70:401–410. [PubMed: 1643658]

Riederer BM, Zagon IS, Goodman SR. Brain spectrin (240/235) and brain spectrin (240. 235E): two distinct spectrin subtypes with different locations within mammalian neural cells. J Cell Biol. 1986; 102:2088–2097. [PubMed: 3519621]

Sandvig K, Olsnes S, Petersen OW, Van Deurs B. Acidification of the cytosol inhibits endocytosis from coated pits. J Cell Biol. 1987; 105:679–689. [PubMed: 2887575]

Scita G, Nordstrom J, Carbone R, Tenca P, Giardina G, Gutkind S, Bjarnegard M, Betsholtz C, Di Fiore PP. EPS8 and E3B1 transduce signals from Ras to Rac. Nature. 1999; 401:290–293. [PubMed: 10499589]

Speicher DW, Marchesi VT. Erythrocyte spectrin is comprised of many homologous triple helical segments. Nature. 1984; 311:177–180. [PubMed: 6472478]

Stankewich MC, Tse WT, Peters LL, Ch'ng Y, John KM, Stabach PR, Devarajan P, Morrow JS, Lux SE. A widely expressed beta III spectrin associated with Golgi and cytoplasmic vesicles. Proc Nat Acad Sci USA. 1998; 95:14158–14163. [PubMed: 9826670]

Swanson JA. Phorbol esters stimulate macropinocytosis and solute flow through macrophages. J Cell Biol. 1989; 94:135–142.

Swanson JA, Watts C. Macropinocytosis. Trends Cell Biol. 1995; 5:424–427. [PubMed: 14732047]

Tse WT, Lux SE. Red blood cell membrane disorders. Br J Haematol. 1999; 104:2–13. [PubMed: 10027705]

Vlahos CJ, Matter WF, Hui KY, Brown RF. A specific inhibitor of phosphatidylinositol 3-kinase, 2-(4-morpholinyl)-8-phenyl-4H-1-benzopyran-4-one (LY294002). J Biol Chem. 1994; 269:5241–5248. [PubMed: 8106507]

West MA, Bretscher MS, Watts C. Distinct endocytic pathways in epidermal growth factor-stimulated human carcinoma A431 cells. J Cell Biol. 1989; 109:2731–2739. [PubMed: 2556406]

Zhou D, Birkenmeier CS, Williams MW, Sharp JJ, Barker JB, Bloch RJ. Small, membrane bound, alternatively spliced forms of ankyrin 1 associated with the sarcoplasmic reticulum of mammalian skeletal muscle. J Cell Biol. 1997; 136:621–631. [PubMed: 9024692]

Ziemnicka-Kotula D, Xu J, Gu H, Potempska A, Kim KS, Jenkins EC, Trenkner E, Kotula L. Identification of a candidate spectrin SH3 binding protein suggests a general mechanism of association of tyrosine kinases with the spectrin-based membrane skeleton. J Biol Chem. 1998; 273:13681–13692. [PubMed: 9593709]
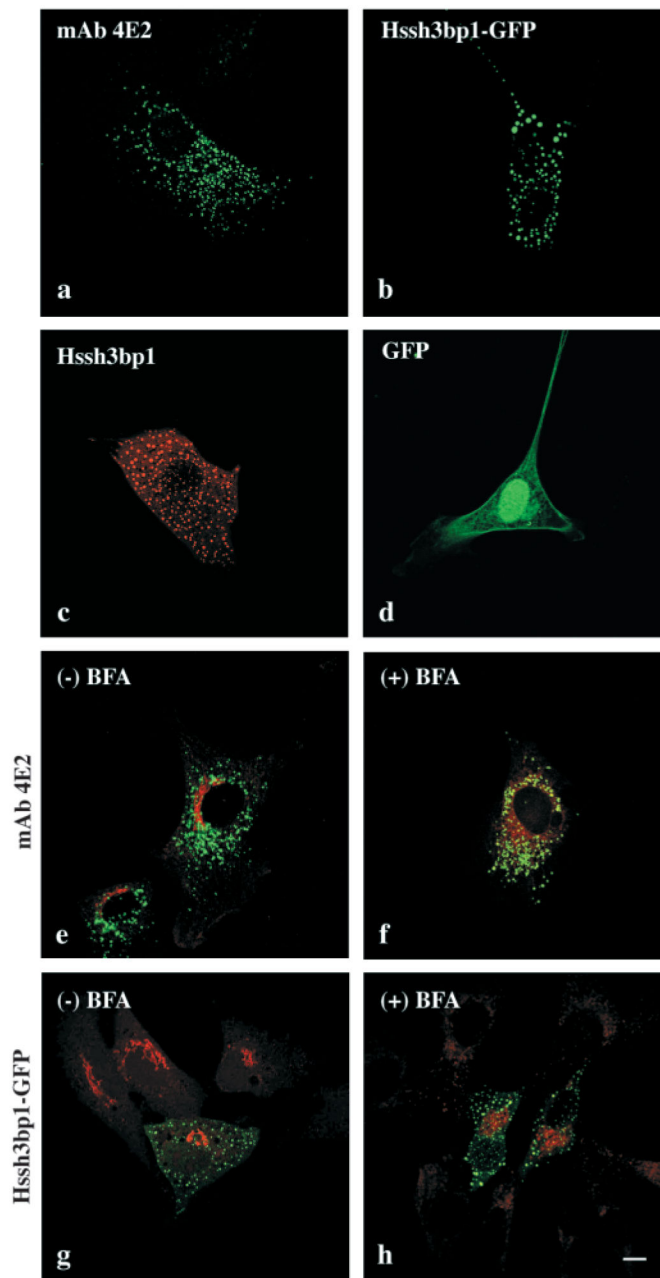
Fig. 1.
Association of Hssh3bp1 and Hssh3bp1-GFP with vesicles resistant to BFA treatment in NIH3T3 cells. (a) Nontransfected NIH 3T3 cell stained with mAb 4E2. (b) Hssh3bp1-GFP-transfected cell. (c) Hssh3bp1-transfected cell stained with mAb 4E2. (d) a cell transfected with GFP alone. (e and f) Cells costained with mAb 4E2 (green) and antibody to mannosidase II (red); (g and h) cells transfected with Hssh3bp1-GFP (green) and costained with antibody to mannosidase II (red). (e and g, f and h) Cells before and after BFA treatment, respectively. Bar, 10 μm.
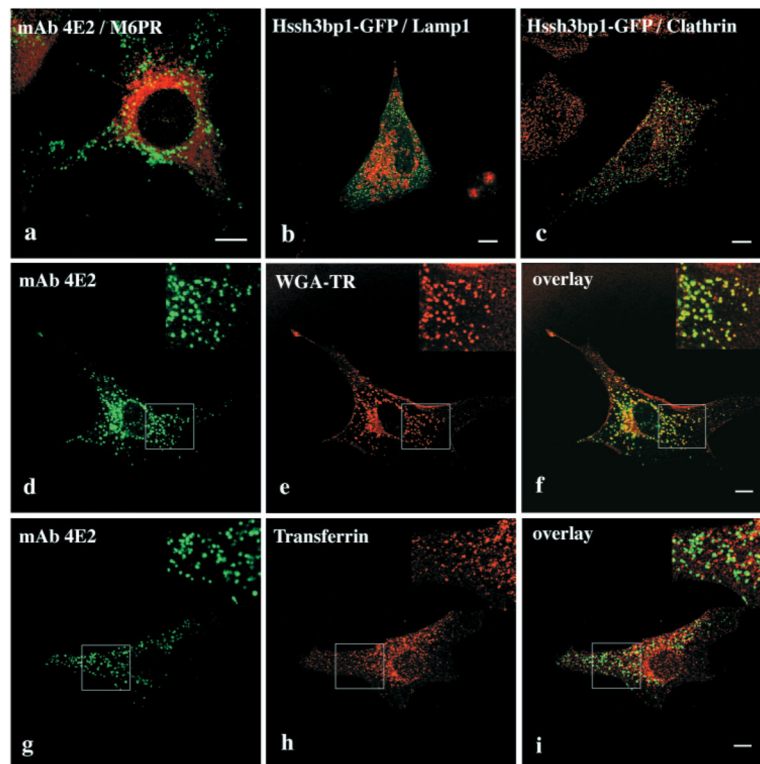
Fig. 2.

Association of Hssh3bp1 with fluid phase non-clathrin coated pinocytic vesicles but not with late endosomes or lysosomes. (a) Costaining of Hssh3bp1 (green) and mannose-6-phosphate receptor (red), a marker of late endosomes. (b) Hssh3bp1-GFP vesicles (green) and lysosomes (red) after bafilomycin A; (c) Hssh3bp1-GFP vesicles (green) do not associate with clathrin (red). (d–f) Cells were allowed to endocytose WGA-TR (red) for 5 minutes and stained with mAb 4E2, (green); (f) an overlay of d and e images. (g–i) Cells were allowed to endocytose transferrin for 5 minutes and stained with mAb 4E2 (green) and with anti-transferrin antibody (red); (i) an overlay of g and h images. Areas in upper right (d–i) of each panel show enlargements of indicated areas. Bar, 10 μm.
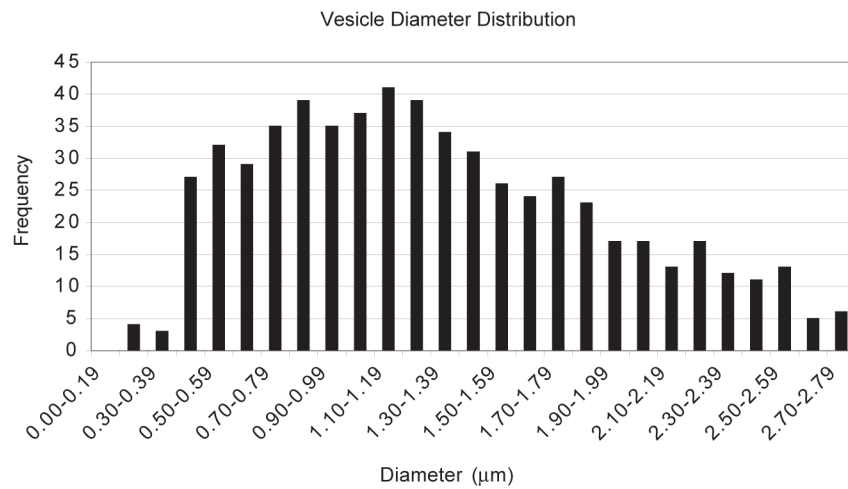
Fig. 3.
Vesicle diameter measurements of Hssh3bp1 vesicles. Vesicle diameter distribution of 622 Hssh3bp1 vesicles indicates a range of 0.5–2.0 µm in size. Measurements were performed using confocal microscopy following staining of NIH 3T3 cells with mAb 4E2 to Hssh3bp1.
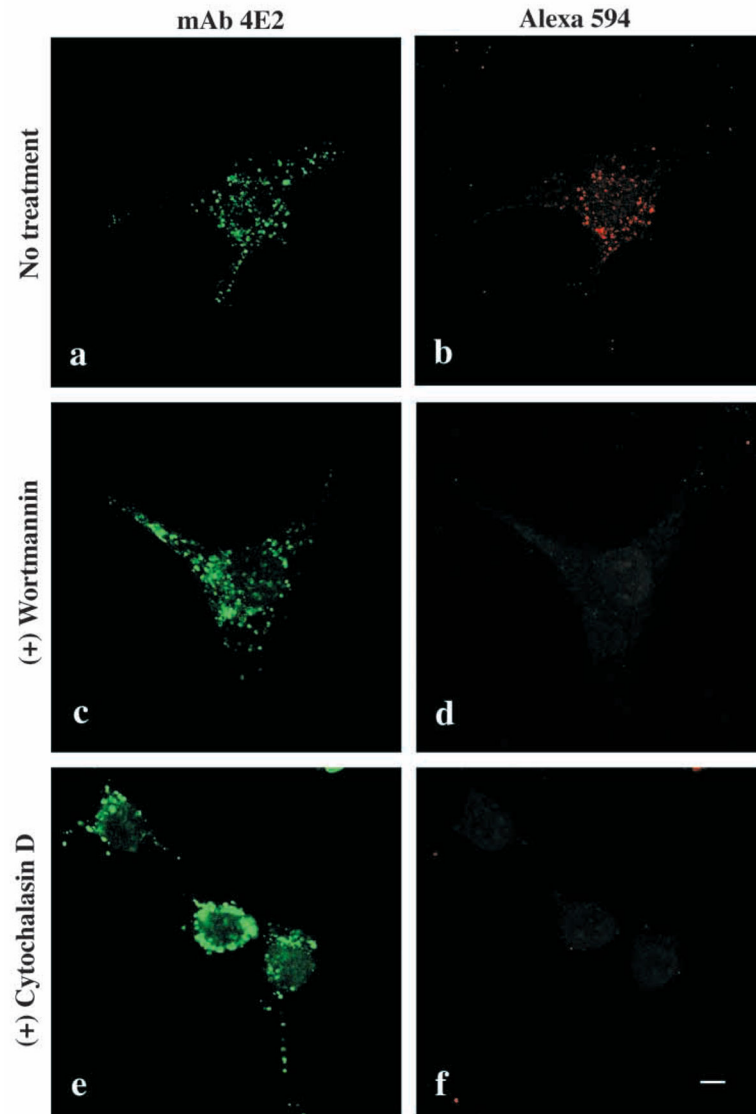
Fig. 4.
Regulation of Hssh3bp1 endocytosis. Endocytosis of Alexa 594 into Hssh3bp1 vesicles (a and b) is abolished by treatment of cells with wortmannin (c and d); cytochalasin D (e and f). Cells were stained with mAb 4E2 (a,c,e) and treated with the respective reagents before Alexa 594 endocytosis (b,d,f). Bar, 10 μm.
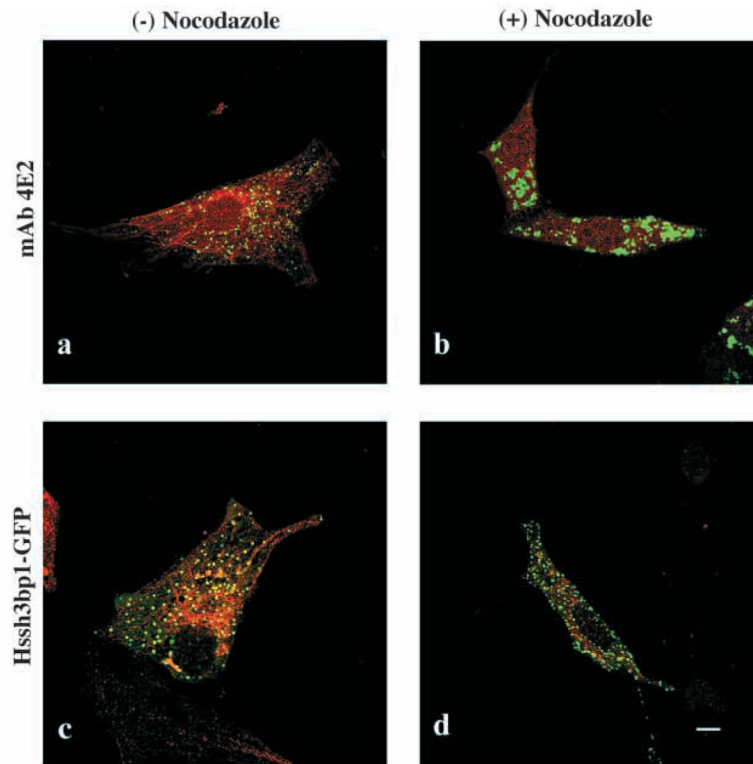
Fig. 5.
Effect of nocodazole treatment on Hssh3bp1 and Hssh3bp1-GFP vesicles. Cells were stained with anti-tubulin (red; a–d) and either costained with mAb 4E2 (green; a and b) or transfected with Hssh3bp1-GFP (c and d). (a and c) Cells before nocodazole treatment; (b and d) cells after nocodazole treatment. Bar, 10 µm.
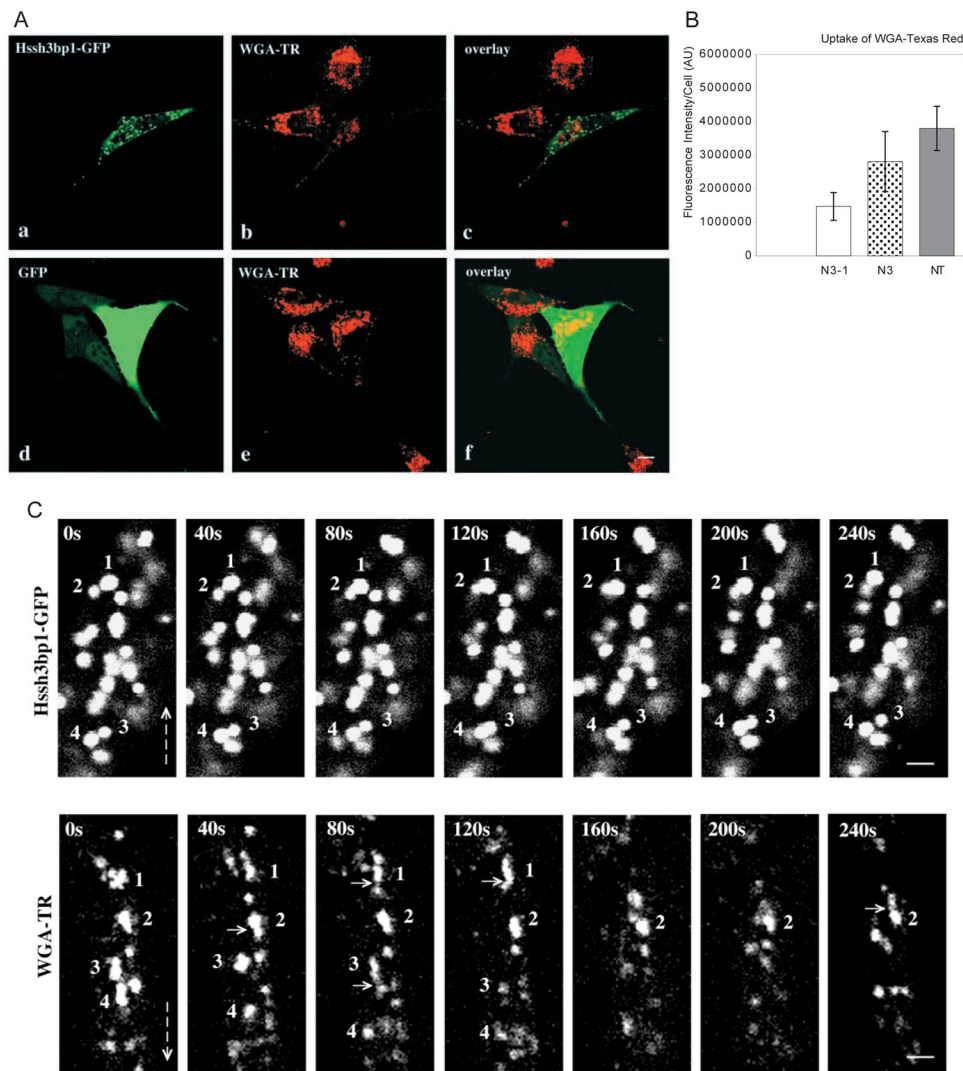
Fig. 6.
Effect of Hssh3bp1-GFP overexpression on endocytosis of WGA-TR in NIH 3T3 fibroblasts. (A) Confocal images were obtained from cells expressing Hssh3bp1-GFP (a and b), or GFP only (d and e). (a and d) Green fluorescence of GFP proteins; (b and e) red fluorescence of WGA-TR. (a and b, d and e) Represent confocal images from the same cells, respectively; (c) an overlay of a and b images; (f) an overlay of d and e images. Note that the cell expressing Hssh3bp1-GFP (the cell in the center of b), endocytosed less fluorescence than nonntransfected cells (cells at the top of b and in the left of b). Bar, 10 μm. (B) Measurements of endocytosed fluorescence in cells transfected with Hssh3bp1-GFP (N3-1), with GFP only (N3), and nonntransfected (NT). In each group not less than 20 individual cells were analyzed (bar represents mean ± s.d.). Similar results were obtained in three independent experiments. (C) Sequential confocal images from a live cell transfected with Hssh3bp1-GFP (upper plates) or from a nontransfected cell (WGA-TR) (lower plates) following uptake of WGA-TR. Images were captured every 40 seconds for 240 seconds. Hssh3bp1-GFP plates: Vesicles 1 and 2, and vesicles 3 and 4, move towards each other,

their images overlap, and then they separate. WGA-TR plates: note formation of short tubules from irregularly shaped structures 1 and 3 (compare 1 at 0 seconds and 40 seconds, and 3 at 40 seconds and 80 seconds). Some possible budding or fusion events are indicated by short arrows. Emergence of peripheral structures which then move towards structure(s) located closer to perinuclear area is common (see structures located above vesicles 1, frames 40 seconds through 120 seconds, and vesicle 2, frames 160 seconds through 240 seconds). Vesicle 4 moves downwards in first four frames. Vertical arrows indicate direction towards perinuclear area of cells. Note substantial morphological changes of WGA-TR vesicles in subsequent frames in comparison to little changes in Hssh3bp1-GFP vesicles. Bar, 2 μm.
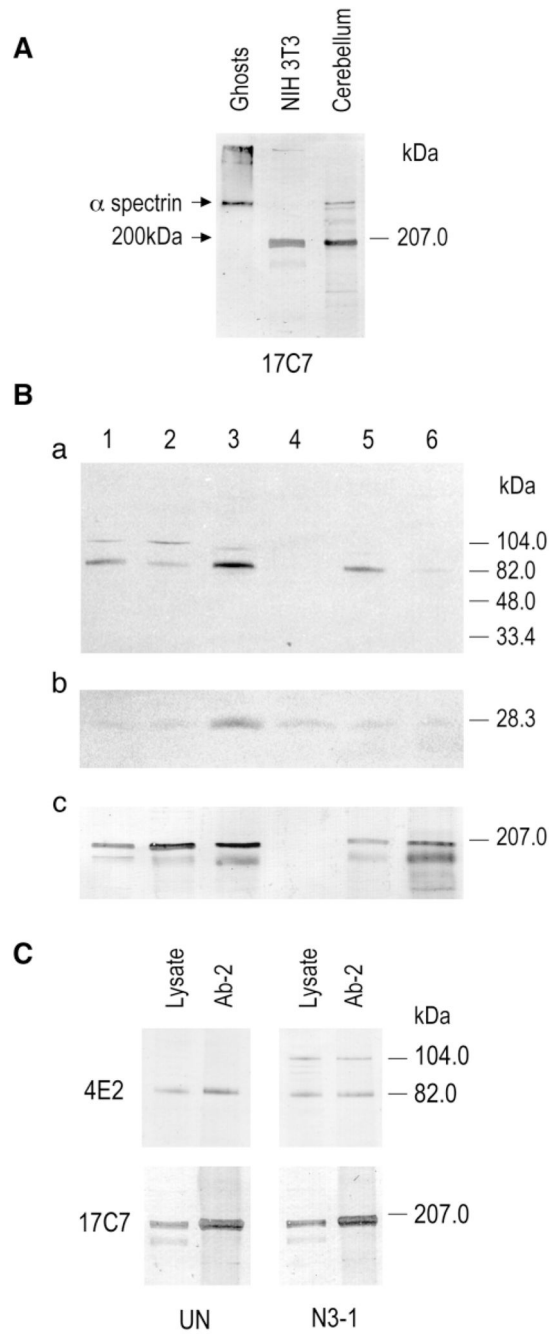
Fig. 7.
Hssh3bp1 interacts with a 200-kDa protein in NIH 3T3 cells. (A) mAb 17C7 raised to the recombinant spectrin SH3 domain reacts with α-spectrin in mouse ghosts and cerebellum, and with a 200-kDa protein in NIH 3T3 cells and cerebellum. (B) Enrichement of Hssh3bp1 vesicles in an early endosomal fraction of NIH 3T3 cells. Equal protein amounts of subcellular fractions were solubilized in Laemmli buffer and separated on SDS-Tricine polyacrylamide gels. Blotted transfers were probed with the polyclonal antibody Ab-2 to Hssh3bp1 (a); with polyclonal antibody to Rab 5a (b); and with mAb 17C7 to the spectrin

SH3 domain (c). Lane 1, total homogenate fraction; lane 2, post-nuclear supernatant fraction; lane 3, early endosomal fraction; lane 4, late endosomal fraction; lane 5, heavy membrane fraction; lane 6, endoplasmic reticulum fraction. Hssh3bp1 and the 200-kDa protein were enriched in the early endosomal fraction (as indicated by presence of Rab 5a and the highest activity of endocytosed HRP after 5 minutes uptake). (C) Hssh3bp1 and Hssh3bp1-GFP coimmunoprecipitating with the 200-kDa protein from NIH 3T3 cell lysates. Lanes represent starting lysates (lysate) and immunoprecipitates obtained with the polyclonal antibody Ab-2 to Hssh3bp1 (Ab-2). Western blots were developed with mAb 4E2 to Hssh3bp1 (upper panel) and mAb 17C7 to the 200-kDa protein (lower panel). UN and N3-1, represent wild-type and Hssh3bp1-GFP-transfected NIH 3T3 cells, respectively.
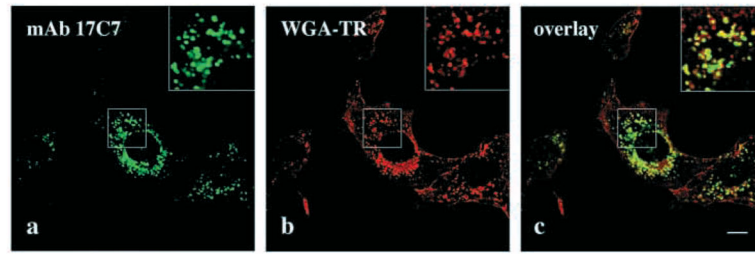
Fig. 8.
mAb 17C7 to the erythroid α-spectrin SH3 domain stains macropinocytic vesicles in NIH 3T3 cells. (a–c) Cells were allowed to endocytose WGA-TR (red) for 5 minutes and stained with mAb 17C7, (green); (c) an overlay of a and b images. Boxed areas in upper right (a–c) of each panel show enlargements of indicated areas. Bar, 10 μm.